Optical Phase Change in Bismuth Through Structural Distortions Induced by Laser Irradiation

Ørjan S. Handegård[1,2], Masahiro Kitajima (北島正弘)[1], and Tadaaki Nagao (長尾忠昭) [1,2,*]

[1]*International Center for Materials Nanoarchitectonics (MANA), National Institute for Materials Science (NIMS), 1-1 Namiki, Tsukuba, Ibaraki 305-0044, Japan*

[2]*Department of Condensed Matter Physics, Hokkaido University, Kita, Sapporo, Hokkaido 060-0808, Japan*

**E-mail: NAGAO.Tadaaki@nims.go.jp*

ABSTRACT

Semimetal Bismuth (Bi) is known to posess a wide range of peculiar properties, owing to its unique electronic band structure. Its electronic band can easily be distorted by structural changes, and thereby undergo transitions between semimetal to either semiconductor or metal states. Utilizing a focused laser beam, one can easily introduce structural defects, along with phase changes, oxidation, and morphological modifications. Confocal Raman microscopy indicated that the as-fabricated Bi droplets inhibit the Raman signal from the underlying silicon (Si) substrate. After a laser flash heating step, the intensity of Si optical phonons was strongly enhanced at the positions of Bi droplets, and exceeding the intensity from the bare Si substrate. Thus, such laser irradiating step on the Bi droplets induces an optical phase change. The optical phase change was detected as going from inhibition to strong enhancement of the underlying Si substrate Raman signal. From the observed Bi optical phonon modes (E_g and A_{1g}), alterations in the Raman peaks due to laser exposure indicated that the ordered crystallinity in pristine Bi droplets became deteriorated. The effects of atomic displacements and loss of structural order in Bi droplets impacts its dielectric response. The observed Si Raman signal enhancement is similar to the surface-enhanced Raman scattering effect typically known for noble metals.

Keywords: bismuth, phase change, laser irradiation, structural defects, Raman spectroscopy

1. Introduction

Bismuth (Bi) belongs to the semimetals in Group V which is a class known for its diversity of allotropes depending on factors such as pressure, temperature, and their crystal growth conditions. With its fascinating and varied properties, Bi has been an extensively studied model material in condensed matter physics, showing unique electronic, mechanical, and optical properties. Many important physical phenomena have been discovered in Bi where its stands out compared to other materials for attributes such as high magnetoresistance, high Seebeck coefficient, low free carrier density, long mean free path, and it has large diamagnetism and complex transport [1,2]. All these varied and unique features of Bi make this material attractive for a wide range of applications within fields, such as magnetic field sensing [3], photocatalysis [4], thermoelectrics [5], and photodetection [6]. These properties are determined by its electronic band structure, and can be influenced by small alterations in crystal structure as well as chemical dopant effects. The crystal state of Bi and its dependence on pressure and temperature is well depicted in the rich phase diagram shown in Figure 1, and shows how sensitive the crystal structure of Bi can be to external stimuli [7]. At standard conditions, the crystal phase is the A7 structure existing in the Bi-I area of the diagram, representing the rhombohedral crystal structure of Bi. The rhombohedral A7 crystal structure can be viewed as a cubic structure which gets slightly distorted due to dimerization, which lowers the overall energy of the system, but breaks the perfect symmetry of the simple cubic lattice. This psudo-cubic equilibrium state gives Bi both a covalent and metallic nature in its bonding characteristics. Phase transitions can be induced relatively easy, by applying a small amount of pressure, Bi-I transforms into monoclinic Bi-II, or turns liquid at low temperature (271 °C melting point for bulk Bi) [8]. When it comes to melting and solidification, these transitions with respect to temperature depend on crystal size, where smaller size is attributed to lowering of melting points. Such surface pre-melting phenomenom has been shown to appear in thin Bi films at temperature of

350 K [9] and many allotropes exist for thin films [10]. Additionally, supercooling effects when cooled from temperatures above the melting point is also known to occur for Bi thin films [11].

As with many materials, any distortions of the crystal structure lead to alterations in the subtle band overlaps near the Fermi level, E_F. This is especially the case for Bi, where crystal distortions can greatly impact its physical properties. The electronic band diagram of Bi is rich and complex, as shown in Fig. 2, and it is characteristic for having a narrow band gap (~15 meV). The characteristic energy overlapping Fermi pockets of Bi for confinement of electron and holes are also highlighted in Fig. 2. The band structure is responsible for giving its carriers small effective mass, high mobility and non-parabolic dispersion [1]. Employing physical methods, such as applying heat and/or pressure (as mentioned above) or chemically by doping and alloying, the electronic band structure can be altered. Such band structure changes can introduce valence- and conduction band overlaps and therby alter the available free carrier concentration, or open up for energy band gaps. As for structural changes, such as atomic internal displacement (defined as *u*) and strain have been studied theoretically on how they can alter the electronic band and induce phase transitions [12–14]. Figure 3 shows how even relatively small atomic displacements along the trigonal axis can introduce transitions from semimetal to either semiconducter or metal. These transitions predict existence of direct- and indirect narrow band gap semiconducting states as well as a metallic state of Bi [12,13]. Introducing structural deformities in Bi intensionally could be a potential route to modify its electronic and optical properties. In the case for completely disordered Bi, i.e. amorphous state, the available free carrier density is four-orders of magnitude greater than the ordered crystalline semimetal Bi [15]. The amorphous Bi shares similar characteristics with its liquid state in terms of its electrical and optical response, and has roughly the same free carrier density and a more metallic character compared to the ordinary A7 crystalline structure [15,16]. Transitions like these can also be induced through chemical methods. A well-known example for semimetal-semiconductor transition is by alloying Bi with Sb. Depending on the Bi:Sb ratio, the relative position of the L and T point bands can be shifted and inverted with varying band gap [17].

Knowing how the properties of Bi can be tuned by introducing defects, still there has been little efforts to explore the potential that Bi has in this manner. These type of structure dependent traits are highly benifical for materials such as optical phase change materials. As for optical phase change materials, the GST alloy materials (Germanium, Antimony, and Telluride) are thoughroughly studied and utilised in memory- and storage based devices [18–20]. A typical attribute for these materials is the capability of tuning optical properties by transforming the crystal structure and switching between different phases of the material, for example between crystalline and amorphous. These transitions are commonly induced by laser irradiation. This optical phase change process is shown in Figure 4, where the refractive index (*n*) and extinction coefficient (*k*) of a typical GST material is given for its corresponding phases. At certain wavelengths, the phase transition from crystalline to amorphous is causing a major change in optical response with respect to *n* and *k*. Regarding the optical properties of Bi, looking at the real part of the permittivity given in Figure 5, it exhibits a metal-dielectric duality in terms of its optical response and has a high refractive index in the long wavelength limit as well as plasmonic characteristics from the near-infrared to the ultraviolet spectral region [21]. The plasmonic behaviour of Bi has been reported [22], and so has the demonstration of surface-enhanced Raman scattering (SERS) for Bi nanoparticles [23]. Another aspect which is an important message to take from the permittivity, is how greatly the reported optical responses differ from one another[21]. This can largely be understood in terms of sample quality differences, and demonstrates how changes in the crystal structure of Bi can affect its interaction with light.

Regarding the use of laser techniques, they offer a powerful and effective way to change material properties and/or structural features. Utilising laser beams for nanofabrication has become of greater importance, such as for tailoring nanoparticles and surface structuring, and it gives accurate control down to sizes is limited only by the spot size of the laser beam and wavelength [24,25]. For Bi, selective laser irradiation can promote oxidation processes [26–28], create micropatterns [29] or form nanoparticles by laser ablation [23,30]. ~~How high power laser~~

~~processing affects the internal structural features, and correspondingly electrical and optical properties, of Bi are not much reported and will be useful investigate as Bi may offer unexplored potential with respect to phase change tunable properties.~~ Reports on how high power laser processing affects the internal structural features, and correspondingly electrical and optical properties, of Bi are lacking. Thus it is therefore of our interest to investigate laser effects in Bi, as it may offer unexplored potential with respect to phase change tunable properties.

Here, we focus on a laser induced change in optical response of Bi, first reported in [31], leading to an enhancement of Raman signal intensity from silicon (Si) substrate positioned underneath Bi droplets. By using spatially resolved confocal Raman microscopy, optical phonon intensity maps of Bi and Si were constructed. Comparison before and after exposure to high power laser irradiation show an striking increase in intensity of Si optical phonons at the exact position of Bi droplets. Substantial changes in Bi E_g and A_{1g} modes were also detected. Furthermore, features in our dark-field microscopy spectra shifted to shorter wavelengths after the laser flash heating of droplets. Our results suggest that an optical phase change was induced when the Bi droplets were subjected to the laser flash heating step. The modified Bi droplets showed an optical response similar to the SERS effect, but enhancing signal from the underlying substrate rather than adsorbed molecules. We can tie this optical modulation to an increasing metallic nature in Bi due to internal structural distortions.

2. Experimental

All experiments and characterization were executed at standard ambient temperature and pressure unless otherwise stated. The experimental details are described in more depth in [31].The Bi droplets were prepared from a Bi thin film on a silicon substrate. The high quality thin films were grown by molecular beam epitaxy (MBE), at a base pressure below 10^{-9} Torr, on a reconstructed Si(111)-7×7 surface [32,33]. The as-deposited films were subjected to a shock post-annealing *in situ* at roughly 300 °C, through resistive heating of the Si substrate. The quality of thin film growth and

effect of resistive heating processes were monitored by recording the respective reflection high energy electron diffraction (RHEED) patterns.

A multifunctional alpha300 system (WITec) was used to perform main parts of Bi droplet experiments and characterisation, including confocal Raman microscopy, atomic force microscopy (AFM), and bright-field- and dark-field microscopy. For the laser irradiation process of the Bi droplets, a confocal setup together with a 785 nm diode laser (Xtra II, Toptica) operated at 30 mW. The laser was focused to a ~2 μm diameter spot, and an area of size 25×25 μm was scanned and exposed to the high power laser irradiation. The Bi droplets before and after laser irradiation were characterized by scanning electron microscopy (SEM; SU8230, Hitachi) and AFM. The AFM topographic information was acquired in tapping mode. AFM image processing, consisting of standard flattening procedures, was done in Gwyddion [34]. For the Raman spectroscopy, a Bragg grating coupler and a 532 nm Nd:YAG continuous wave laser source were used. The laser was focused to a spot diameter of ~1.5 μm and operated at 6 mW. Raman spectra were acquired across the selected area before and after high power laser irradiation. Optical phonon images were constructed by Raman peak integration with background subtraction using Project FOUR (WITec). Light scattering from the Bi droplets was characterized by reflection dark-field microscopy, using a white halogen lamp as the illumination source.

3. Results and Discussion

3.1 Preparation and characterization of Bi droplets

A schematic of Bi droplets formation with characterization by RHEED and SEM is shown in Figure 6a. The high surface sensitivity of RHEED technique provides detailed insight into sample crystallinity by observation of diffraction lines and spots on a fluorescent screen. The streaky lines seen in the RHEED pattern (Fig. 6b) are recognized as Bi single crystalline thin films with its trigonal axis normal to the surface plane ([001] orientation) [32,33]. When applying current across the Si substrate to initiate resistive heating, the thin film integrity and geometry became disrupted,

and went from a continuous 2D film to disconnected 3D droplets. This process was tracked by monitoring the RHEED pattern, which changed from its streaky lines to a spotty transmission pattern as 3D structures formed (Fig. 6d). The formation of 3D structures in the form of droplets from the thin film was confirmed by SEM, after the resistive heating, droplet shapes of Bi were clearly visible (Fig. 6c and e). The resistive heating process resulted in a thermal dewetting of Bi, as the film spontaneous develops into droplets on the Si surface to minimize contact area, as occurs when a molten film with high surface tension resolidifies [35,36].

Images from a selected region of interest were captured by optical bright-field microscopy, SEM, and AFM before and after exposure to the high-power focused laser beam (785 nm), referred to here as laser flash heating (Fig. 7). Before laser flashing, the pristine Bi droplets were smooth, hemispherical, and separately distributed throughout the substrate (Fig. 7b, c and d). After the laser flashing step (Fig. 7e, f, and g), the appearance and morphology of the droplets changed compared with their original features. From the bright-field images, all the laser-exposed droplets appeared darker and the larger droplets widened (Fig. 7b and e). In the SEM images (Fig. 7c and f), the smaller droplets (< 1 μm) were less affected by laser exposure; however the height of larger droplets decreased and smaller particles appeared around them. These observations suggest that "volatile boiling" occurred during the laser flash heating step. These observations are furthermore supported by AFM results (Fig. 7d and g).

3.2 Si Raman signal enhancement

We used spatially resolved Raman microscopy to investigate any modifications to the inherent features of the Bi droplets after high-power laser exposure. Raman spectra from a single Bi droplet, under pristine and laser-flashed conditions, were obtained respectively with Si substrate signal subtracted (Fig. 8b). From the Raman spectra, the two first-order optical phonon modes, E_g (transverse) and A_{1g} (longitudinal), of Bi modes were observed at 67 cm^{-1} and 92 cm^{-1}. Spatially resolved phonon images of Si (520 cm^{-1}) are given in Fig. 8c and d before and after laser exposure

respectively. In the pristine case, the Raman signal from the Si substrate was much weaker at the droplet position compared to the bare Si substrate (i.e. peak intensities at Bi positions were lower than the bare Si substrate). After the laser flash step, the Si Raman peak intensity increased remarkably, and became much greater at the position of Bi droplets than at the Si substrate. This change in optical response of Bi is evident when looking at the Raman intensity maps. First (Fig. 8c), where Si Raman signal was quite weak (dark regions) where Bi A_{1g} signal was strong (bright regions). This observation indicates that the presence of Bi inhibits Raman scattering from the substrate. On the contrary, for laser flashed droplets (Fig. 8d), the intensity of the Si optical phonons increased greatly at the position of Bi (bright regions). This sharp increase in the Si Raman signal suggests that the laser flashing step presumably alters the nature of Bi droplets such that its carrier density and the optical response enhances the local electromagnetic field in proximity to the droplets and hence the signal from the substrate.

3.3 Structural distortions in Bi induced by high power laser irradiation

The Raman microscopy measurements of Bi droplets were furthermore analyzed to reveal any modifications in the structural integrity. From the scattered light detected by Raman spectroscopy, insight into vibrational modes, and details such as crystal phase, stress, and structural point defects can be gathered [37]. By examination of Raman peak intensities and linewidths of the Bi optical phonon modes, we can discuss any structural changes occurring in the droplets after the laser-flashed heating step. Raman spectra obtained from a single Bi droplet, for pristine and laser-flashed condition, are given in Fig. 9a. The Raman peaks for the E_g and A_{1g} optical phonon modes of rhombohedral Bi were detected at 67 cm^{-1} and at 92 cm^{-1}, respectively. The two-fold degenerate E_g transverse optical mode is produced by atomic displacement occurring within the plane of the Bi bilayer (parallel with the (001) crystal plane). The displacement of the symmetric A_{1g} longitudinal mode occurs in between the bilayers (along the [001] trigonal axis), as shown in Fig. 9~~c~~b. The sharp Raman peaks of the E_g and A_{1g} modes indicate that the pristine droplets were highly crystalline, and

the E_g signal was approximately twice as intense as the A_{1g} signal (Fig. 9a). On the other hand, after high-power laser irradiation, the E_g and A_{1g} signals exhibited a comparable intensity and their peak width broadened considerably. Because of the sensitivity of Raman spectroscopy to crystallinity and symmetry of the crystal lattice, these peak changes indicate a change in the preferential structure orientation of the laser flashed droplets compared with the pristine droplets. The relative peak intensity between optical phonon modes is useful as an indicator for studying disorder and phase changes, and has been frequently used for determining defects in and phase of carbon materials and others [38–40]. For example, Raman peak broadening in Bi correlate with crystal point defects, as has previously been shown for the A_{1g} mode where the vibrational decay rate/damping increases as more defects are introduced [41]. For our Raman spectra, by applying Lorentzian peak fitting to the observable Bi phonon modes, we measured full-width at half-maximum (FWHM) broadening from 14.2 to 25.6 cm^{-1} and a frequency shift from 66.7 to 68.1 cm^{-1} for the E_g mode. For the A_{1g} mode, we observed a FWHM broadening from 13.1 to 24.8 cm^{-1} and a frequency shift from 92.6 to 91.8 cm^{-1}. The intensity ratio of E_g/A_{1g} decreased from 2.07 to 0.99. The peak shifts, broadening, and E_g/A_{1g} intensity ratio change for the laser flashed Bi droplets suggest: I) deterioration of long-range translational symmetry by introduction of defects. II) changes in the local bonding character, induced by the laser exposure. Possibly, the rapid heating and subsequent cooling exerted by the high-powered laser transformed the crystalline Bi microdroplets into a more disordered state, closer to an amorphous- or liquid-like state. This distortion can increase the metallic character of Bi, as mentioned above, because minute electronic band overlaps are largely affected when atoms are displaced. Since the band overlaps are rather small, only subtle changes in the electronic band structure can cause a tremendous change in its electrical and optical properties. Furthermore, not only is atomic displacement reported to increase available carrier density [13], but also both amorphous and liquid state are reported to have a metallic character with much higher free carrier concentration [15,16]. In the next subsection we will discuss in more detail how these structural and electronic changes affect the optical response. Another observation from the Raman spectra of the

laser irradiated droplets is the appearance of two new peaks, indicating the formation of bismuth oxide (Bi_2O_3). Many phases of Bi_2O_3 exist, however, only the β-Bi_2O_3 phase was reported to form through laser flashing, which was confirmed by the peak positions at 125 and 314 cm^{-1} characteristic of β-Bi_2O_3 [27,28]. According to preceeding work, the onset of β-Bi_2O_3 formation under ambient conditions takes place only above the melting point of Bi [27]. Thus, the observation of β-Bi_2O_3 formation confirmed that Bi droplets underwent local melting and resolidification caused by the high power laser flashing step.

3.4 Laser induced optical phase change in Bi

To further investigate the correlation between the structural transition in Bi droplets and observed strong Raman signal enhancement of Si, we collected dark-field microscopy spectra and constructed spectral images from scattered white light by pristine and laser flashed Bi droplets, as shown in Fig. 10. The dark-field spectra exhibited clear feature in the visible to the near infrared region, and their peak positions shift to lower wavelengths after the laser-flashing of Bi droplets (Fig. 10d). We attribute the predominant contribution these spectral shifts to lower wavelengths with an increase in the free carrier concentration. Because the morphology was not markedly changed after laser flashing, based on AFM and SEM observations, a change in the available carrier density, as discussed above, would be the most possible contributing factor to the altered scattering properties of the laser flashed Bi droplets. As previously reported, atomic displacements and disordering would alter the carrier concentration [12,13]. Such is indicative of changes in electronic structure, which we observe as modulation in optical response, i.e. an optical phase change.

Based on the presented results above, we discuss the origin of the Si Raman signal enhancement by laser flash heated Bi droplets on the Si substrate. The rapid melting and resolidification most possibly transforms the droplets from a crystalline to a disordered state. In the case of disordered Bi, it is expected that it becomes more metallic in nature as its amorphousness or disorder increases [13,15]. The droplets would then share similarities partly with amorphous and

liquid Bi, which both have much higher density of carriers and are metallic in nature [15,16]. Another similarity between amorphous and liquid Bi, is that their optical response (dielectric function/permittivity) can be described by the Drude model [15,16], meaning that the free carriers are dominating the materials response to electromagnetic radiation. Regarding metal-liquid transition of Bi, a recent report shown that at the transition from solid to liquid phase, the real part of the dielectric function (ε_1) becomes more negative and the imaginary part (ε_2) increases [16]. When the crystalline structure of semimetal Bi becomes distorted, subtle overlap between the valence and conduction band is modified, leading to a sharp increase in metallic character and an altered electrical and optical response. In other words, the absorption coefficient and refractive index of Bi are strongly influenced by the state of its crystal lattice. These arguments can consistently explain our findings, where in the Raman spectra we detected a lattice disorder in Bi, strong enhancement in Si phonons beneath the Bi droplets, as well as blueshifts in dark-field scattering spectra, which all occuring only after the laser flash heating step. Especially, the strong enhancenet of Si Raman signal at the position of Bi droplets strongly suggests an optical phase change occurring in Bi. Even though plasmonic behaviour [21] and SERS effect [23] have recently been reported in the literature, these phenomena in Bi are not intuitive and our findings demonstrate that with this semimetal, its internal atomic arrangements can drastically affect its optical response. Given the strong correlation between crystal structure and electronic band structure, this aspect needs to be considered in the future for laser processing of Bi materials. As our findings suggest, the local heating and subsequent melting of Bi droplets, induced by the high-power laser irradiation, are followed by rapid cooling through the Si substrate, which has high thermal conductivity to dissipate the heat. Under these conditions the Bi droplets resolidify with a low degree of crystallinity and end in a state of higher disorder. Lattice disorder will relax the semimetal Bi lattice from an open-packed covalent-like layered lattice to a more close-packed metal-like simple cubic lattice driving it to a more conductive phase. Thus, the laser flashed Bi droplets is transformed into a defect-

containing disordered state with properties closer to those of liquid or amorphous Bi, which have metallic rather than semimetallic characteristics.

Our observations of an optical phase change in Bi, and the strong Si Raman signal enhancement can be related to SERS effect originated from a plasmon associated carrier response in the laser flash heated Bi droplets. Such laser processing of nano-/microscale objects, especially for Bi and other semimetals, will open a new way to tailor optical and electrical functionality of materials.

4. Conclusions

Semimetal Bi is an exotic material which has a rich phase diagram and unique electronic structure that is highly sensitive to changes in its crystal structure. Knowing this, Bi offer unexplored potential for phase change materials and can be an ideal material for laser processing. Here, we focused on a system of well-defined Bi droplets prepared on a Si(111) substrate by thermal dewetting of an epitaxially grown thin film. By subjecting the pristine droplets to a laser flash heating step, a drastic change in their dielectric response was observed by spatially visualized by Raman microscopy, as well as dark-field microscopy. After laser flashing, the Si Raman signals increased markedly at the position of Bi droplet compared to inhibiting the Si Raman signals in the pristine case. Such change in Raman spectra indicate that the droplets underwent an optical phase change from inhibiting to enhancing the Raman signal intensity of underlying Si substrate in contact with them. The white light scattering spectra of Bi droplets, collected by dark-field microscopy, exhibited systematic spectral shifts towards shorter wavelengths after the laser exposure. These observations clearly indicate a change in the optical response of Bi, as it shifted to a highly metallic phase. We propose that this transition in the optical phase arises because of lattice distortions, introduced by melting and quench-cooling by laser flashing, which influence the available carrier concentration of Bi. Our study demonstrates the potential for tailoring the optical response of

nano/micro-scale objects by laser irradiation, which can open new paths of exploration in controlling the optical functionalities of materials.

Acknowledgements

This work is partially supported by JSPS KAKENHI (16F16315, JP16H06364, 16H03820), and CREST "Phase Interface Science for Highly Efficient Energy Utilization" (JPMJCR13C3) from Japan Science and Technology Agency. We are also thankful to S. Ishii, T. D. Dao, and H. D. Ngo for scientific discussions.

References

[1] Y. Fuseya, M. Ogata and H. Fukuyama, *Transport properties and diamagnetism of dirac electrons in bismuth*, J. Phys. Soc. Japan 84 (2015), pp. 54–56.

[2] Z. Zhang, X. Sun, M.S. Dresselhaus, J. Ying and J. Heremans, *Electronic transport properties of single-crystal bismuth nanowire arrays*, Phys. Rev. B 61 (2000), pp. 4850–4861.

[3] K. Liu, P. Searson, F.Y. Yang, K. Liu, K. Hong, D.H. Reich et al., *Yang , F . Y . et al . Large magnetoresistance of electrodeposited single-crystal bismuth thin Large Magnetoresistance of Electrodeposited Single-Crystal Bismuth Thin Films*, 284 (1999), pp. 1335–1337.

[4] J. Li, Z. Wang, F.L. Deepak, H. Qiao, J. Yuan, Z. Xu et al., *An Advanced Semimetal-Organic Bi Spheres-g-C3N4Nanohybrid with SPR-Enhanced Visible-Light Photocatalytic Performance for NO Purification*, Phys. Rev. B 9 (2017), pp. 585–589.

[5] M.S. Dresselhaus, Y.M. Lin, O. Rabin, A. Jorio, A.G. Souza Filho, M.A. Pimenta et al., *Nanowires and nanotubes*, Mater. Sci. Eng. C 23 (2003), pp. 129–140.

[6] J.D. Yao, J.M. Shao and G.W. Yang, *Ultra-broadband and high-responsive photodetectors based on bismuth film at room temperature*, Sci. Rep. 5 (2015), pp. 1–7.

[7] P.W. Bridgman, *Polymorphism, principally of the elements, up to 50,000 kg/cm2*, Phys. Rev. 48 (1935), pp. 893–906.

[8] Z. Liu, G. Shen, B. Xu, Y. Shu, Y. Kono, Y. Wang et al., *Deep melting reveals liquid structural memory and anomalous ferromagnetism in bismuth*, Proc. Natl. Acad. Sci. 114 (2017), pp. 3375–3380.

[9] S. Yaginuma, T. Nagao, J.T. Sadowski, A. Pucci, Y. Fujikawa and T. Sakurai, *Surface pre-melting and surface flattening of Bi nanofilms on Si(1 1 1)-7 × 7*, Surf. Sci. 547 (2003), pp. L877–L881.

[10] T. Nagao, J.T. Sadowski, M. Saito, S. Yaginuma, Y. Fujikawa, T. Kogure et al., *Nanofilm allotrope and phase transformation of ultrathin Bi film on Si(111)-7×7*, Phys. Rev. Lett. 93 (2004), pp. 10–13.

[11] T. Mieko, *Electron-Diffraction Study of Liquid-Solid Transition of Thin Metal Films*, J. Phys. Soc. Japan 9 (1954), pp. 359–363.

[12] A.B. Shick, J.B. Ketterson, D.L. Novikov and A.J. Freeman, *Electronic structure, phase stability, and semimetal-semiconductor transitions in Bi*, Phys. Rev. B - Condens. Matter Mater. Phys. 60 (1999), pp. 15484–15487.

[13] C.Y. Wu, L. Sun, H.R. Gong and S.F. Zhou, *Influence of internal displacement on band structure, phase transition, and thermoelectric properties of bismuth*, J. Mater. Sci. 54 (2019), pp. 6347–6360.

[14] I. Aguilera, C. Friedrich and S. Blügel, *Electronic phase transitions of bismuth under strain from relativistic self-consistent GW calculations*, Phys. Rev. B - Condens. Matter Mater. Phys. 91 (2015), pp. 1–7.

[15] O. Hunderi, *Optical properties of crystalline and amorphous bismuth films*, J. Phys. F Met. Phys. 5 (1975), pp. 2214–2225.

[16] L. Yang, Y.X. Zheng, S.D. Yang, Z.H. Liu, J.B. Zhang, R.J. Zhang et al., *Ellipsometric study on temperature dependent optical properties of topological bismuth film*, Appl. Surf. Sci. 421 (2017), pp. 899–904.

[17] B. Lenoir, M. Cassart, J.P. Michenaud, H. Scherrer and S. Scherrer, *Transport properties of Bi-rich Bi-Sb alloys*, J. Phys. Chem. Solids 57 (1996), pp. 89–99.

[18] M. Wuttig and N. Yamada, *Phase-change materials for rewriteable data storage*, Nat. Mater. 6 (2007), pp. 824–832.

[19] S. Raoux, *Phase Change Materials*, Annu. Rev. Mater. Res. 39 (2009), pp. 25–48.

[20] K.J. Miller, R.F. Haglund and S.M. Weiss, *Optical phase change materials in integrated silicon photonic devices: review*, Opt. Mater. Express 8 (2018), pp. 2415–2429.

[21] J. Toudert, R. Serna, I. Camps, J. Wojcik, P. Mascher, E. Rebollar et al., *Unveiling the Far Infrared-to-Ultraviolet Optical Properties of Bismuth for Applications in Plasmonics and Nanophotonics*, J. Phys. Chem. C 121 (2017), pp. 3511–3521.

[22] J. Toudert, R. Serna and M. Jiménez De Castro, *Exploring the optical potential of nano-bismuth: Tunable surface plasmon resonances in the near ultraviolet-to-near infrared range*, J. Phys. Chem. C 116 (2012), pp. 20530–20539.

[23] A.G. Bezerra, P. Cavassin, T.N. Machado, T.D. Woiski, R. Caetano and W.H. Schreiner, *Surface-enhanced Raman scattering using bismuth nanoparticles: a study with amino acids*, J. Nanoparticle Res. 19 (2017), pp. 362.

[24] K.C. Phillips, H.H. Gandhi, E. Mazur and S.K. Sundaram, *Ultrafast laser processing of materials: a review*, Adv. Opt. Photonics 7 (2015), pp. 684–712.

[25] M. Malinauskas, A. Žukauskas, S. Hasegawa, Y. Hayasaki, V. Mizeikis, R. Buividas et al., *Ultrafast laser processing of materials: from science to industry*, Light Sci. Appl. 5 (2016), pp. e16133.

[26] L. Kumari, J.H. Lin and Y.R. Ma, *Laser oxidation and wide-band photoluminescence of thermal evaporated bismuth thin films*, J. Phys. D. Appl. Phys. 41 (2008), pp. 025405.

[27] J.A. Steele and R.A. Lewis, *Laser-induced oxidation kinetics of bismuth surface microdroplets on GaAsBi studied in situ by Raman microprobe analysis*, Opt. Express 22 (2014), pp. 32261.

[28] C. Díaz-Guerra, P. Almodóvar, M. Camacho-López, S. Camacho-López and J. Piqueras, *Formation of β-Bi2O3and δ-Bi2O3during laser irradiation of Bi films studied in-situ by spatially resolved Raman spectroscopy*, J. Alloys Compd. 723 (2017), pp. 520–526.

[29] A. Reyes-Contreras, M. Camacho-López, S. Camacho-López, O. Olea-Mejía, A. Esparza-García, J.G. Bañuelos-Muñetón et al., *Laser-induced periodic surface structures on bismuth thin films with ns laser pulses below ablation threshold*, Opt. Mater. Express 7 (2017), pp. 1777.

[30] S. Onari, M. Miura and K. Matsuishi, *Raman spectroscopic studies on bismuth nanoparticles prepared by laser ablation technique*, Appl. Surf. Sci. 197–198 (2002), pp. 615–618.

[31] Ø.S. Handegård, M. Kitajima and T. Nagao, *Laser-induced structural disordering and optical phase change in semimetal bismuth observed by Raman microscopy*, Appl. Surf. Sci. 491 (2019), pp. 675–681.

[32] T. Nagao, T. Doi, T. Sekiguchi and S. Hasegawa, *Epitaxial Growth of Single-Crystal Ultrathin Films of Bismuth on Si (111) Epitaxial Growth of Single-Crystal Ultrathin Films of Bismuth on Si (111)*, 4567 (2000), pp. 0–4.

[33] S. Yaginuma, T. Nagao, J.T. Sadowski, M. Saito, K. Nagaoka, Y. Fujikawa et al., *Origin of flat morphology and high crystallinity of ultrathin bismuth films*, Surf. Sci. 601 (2007), pp. 3593–3600.

[34] D. Nečas and P. Klapetek, *Gwyddion: An open-source software for SPM data analysis*, Cent. Eur. J. Phys. 10 (2012), pp. 181–188.

[35] R. Daudin, C. Revenant, G. Davi and G. Renaud, *Growth and dewetting of gold on Si(1 1 1) investigated in situ by grazing incidence small angle x-ray scattering*, Phys. E Low-dimensional Syst. Nanostructures 44 (2012), pp. 1905–1909.

[36] M. Kang, S.G. Park and K.H. Jeong, *Repeated Solid-state Dewetting of Thin Gold Films for Nanogap-rich Plasmonic Nanoislands*, Sci. Rep. 5 (2015), pp. 14790.

[37] M. Cardona, *Light Scattering in Solids I*, Vol. 8, 1983.

[38] M.A. Pimenta, G. Dresselhaus, M.S. Dresselhaus, L.G. Cançado, A. Jorio and R. Saito, *Studying disorder in graphite-based systems by Raman spectroscopy*, Phys. Chem. Chem. Phys. 9 (2007), pp. 1276–1290.

[39] A. Jorio, E.H.M. Ferreira, M.V.O. Moutinho, F. Stavale, C.A. Achete and R.B. Capaz, *Measuring disorder in graphene with the G and D bands*, Phys. Status Solidi Basic Res. 247 (2010), pp. 2980–2982.

[40] P. Colomban and A. Slodczyk, *Raman intensity: An important tool in the study of nanomaterials and nanostructures*, Acta Phys. Pol. A 116 (2009), pp. 7–12.

[41] M. Hase, K. Ishioka, M. Kitajima, K. Ushida and S. Hishita, *Dephasing of coherent phonons by lattice defects in bismuth films*, Appl. Phys. Lett. 76 (2000), pp. 1258–1260.

[42] H. Iwasaki and T. Kikegawa, *Structural Systematics of the High-Pressure Phases of Phosphorus, Arsenic, Antimony and Bismuth*, Acta Crystallogr. Sect. B Struct. Sci. 53 (1997), pp. 353–357.

[43] J. Toudert and R. Serna, *Interband transitions in semi-metals, semiconductors, and topological insulators: a new driving force for plasmonics and nanophotonics [Invited]*, Opt. Mater. Express 7 (2017), pp. 2299.

Figure captions

Figure 1. (a) Phase diagram of Bi with dependence on temperature (K) and pressure (Gpa). The different areas in the phase diagram belong to different phases of Bi. (b) Examples of Bi crystal structures; (I) rhombohedral, (II) monoclinic, (III) tetragonal, and (IV) Body-centered, adapted from [42]. Bi-V phase exists as body-centered cubic (bcc) structure (not shown).

Figure 2. (a) Electronic band diagram of Bi. (b) Highlight of the Fermi pockets located at the L point (electron pocket) and at the T point (hole pocket), showing the energy overlap. The electronic band diagrams, in (a) and (b), are adapted from [1]. (c) The Brillouin zone of Bi.

Figure 3. (a) The two-atom rhombohedral unit cell of Bi viewed in the hexagonal crystal cell. The arrows on the center atom illustrates displacement direction along the trigonal axis. (b) Dependence of internal displacement (u) on the energy band gap as well as band overlap. At specific displacements, Bi exists in semiconducting or metallic states, adapted from [13]. (c) Electronic band diagram of Bi at specific atom displacements. ~~(c) is reprinted with permission from ... [12].~~ (c) Reprinted with permission from A.B. Shick *et al*, Phys. Rev. B 60, 15484 (1999) [12]. Copyright (2019) by the American Physical Society.

Figure 4. (a) Refractive index, *n*, and extinction coefficient, k, of a typical GST material for different phases; hexagonal, rocksalt, and amorphous. (b) Schematic illustration of structural changes between different phases.

Figure 5. Comparison of the real part, ε_1, of the permittivity / dielectric function of Bi from different reports found in the literature. Reprinted with permission from [43]. Copyright 2017 American Chemical Society.

Figure 6. (a) Schematic of Bi droplet formation from a thin film by thermal dewetting. (b) RHEED pattern of MBE grown Bi thin film on Si(111). (c) SEM image of Bi thin film. Scale bar is 0.5 μm. (d) RHEED pattern after thermal dewetting of thin film by resistive heating. (e) SEM image of Bi droplets. Scale bar is 1 μm.

Figure 7. (a) Schematic illustration of the laser flash heating procedure. (b)-(g) Images of Bi droplets in a selected area before and after laser flash heating step. (b),(e) Optical bright-field images. (c),(f) SEM images. (d),(g) AFM images. Scale bar in all images is 5 μm.

Figure 8. (a) Simple schematic of the Raman microscopy setup in this study. (b) Raman spectra from a single Bi droplet, taken before (blue) and after (red) laser flash heating step. Each of the given spectra from the droplets has substracted background intensity from the Si substrate. (c) Constructed 2D map of Si optical phonons (520 cm^{-1}) for pristine condition. (d) Construced 2D map of Si optical phonons after laser flash heating.

Figure 9. (a) Optical phonons of Bi, E_g and A_{1g}, detected in pristine and laser flashed Bi droplets. (b) Schematic of how the laser flash heating step may influence on atomic remodeling within a droplet.

Figure 10. (a) Simple schematic of the dark-field microscopy setup in this study. (b) and (c) Dark-field microscopy image of Bi droplets before and after laser flash heating step, respectively. (d) Dark-field microscopy spectra obtained from individual Bi droplets, as indicated in (b) and (c).

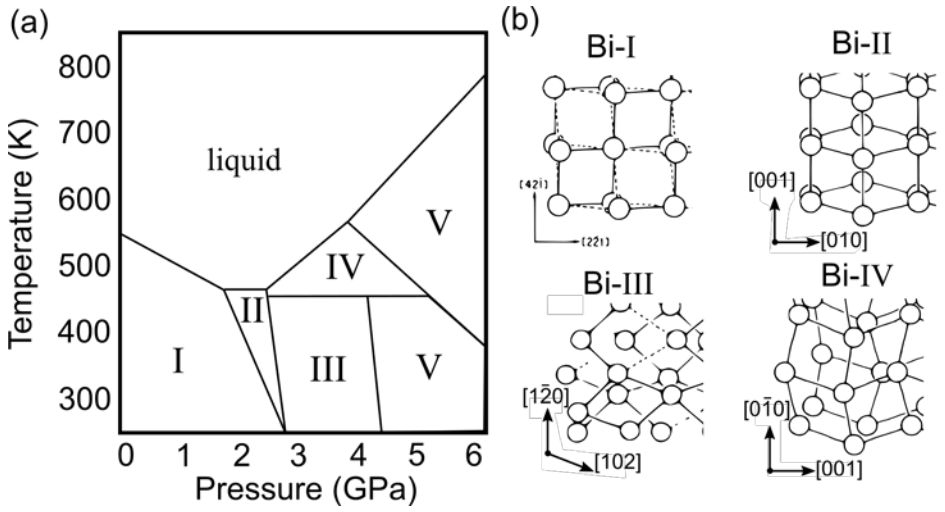

Figure 1. (greyscale) Ø. S. Handegård *et al.*

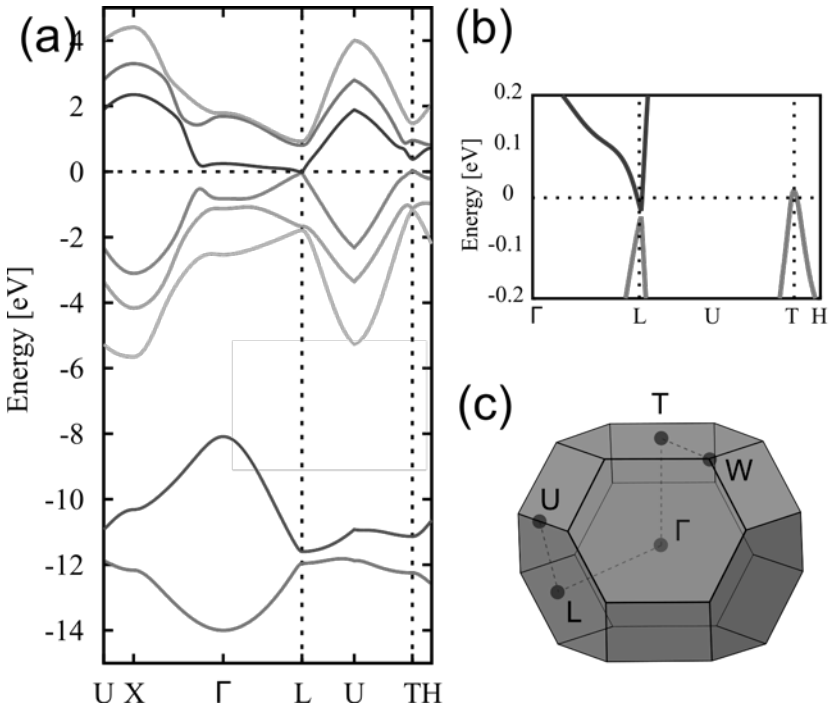

Figure 2. (greyscale) Ø. S. Handegård *et al.*

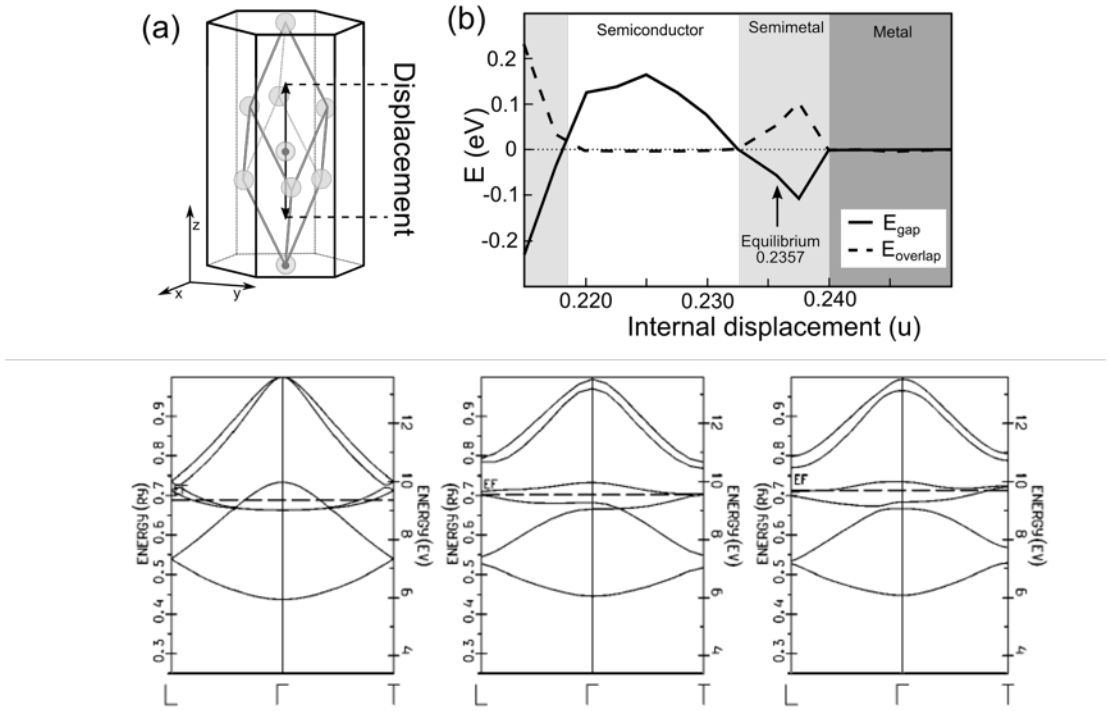

Figure 3. (greyscale) Ø. S. Handegård *et al.*

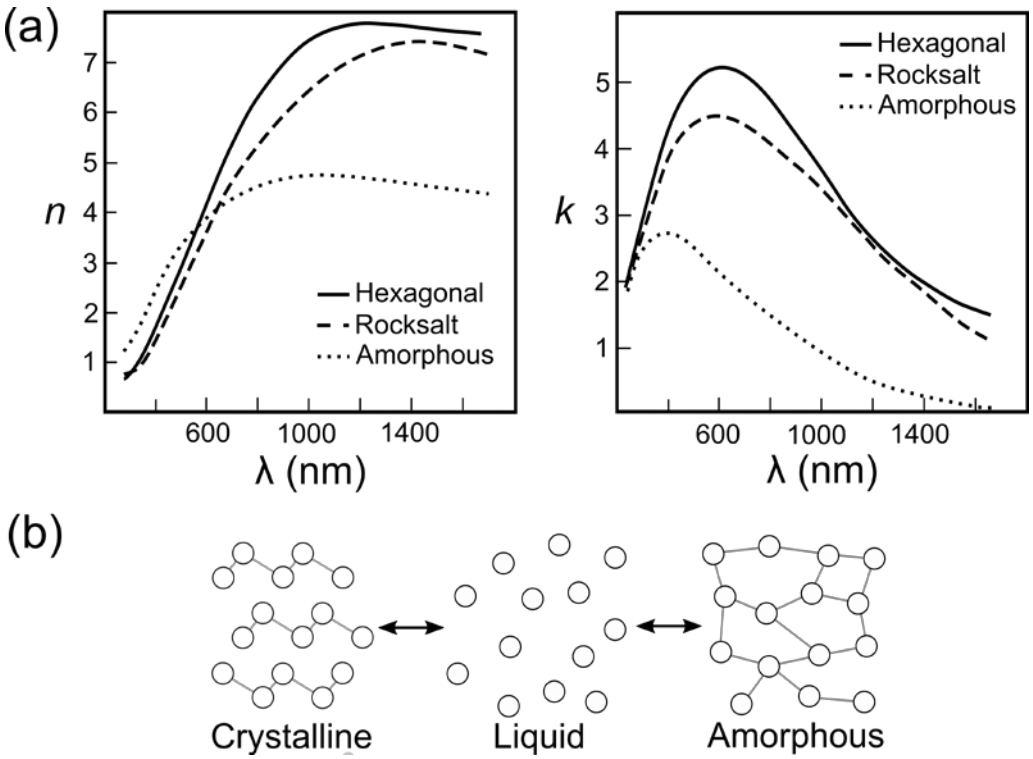

Figure 4. (greyscale) Ø. S. Handegård *et al.*

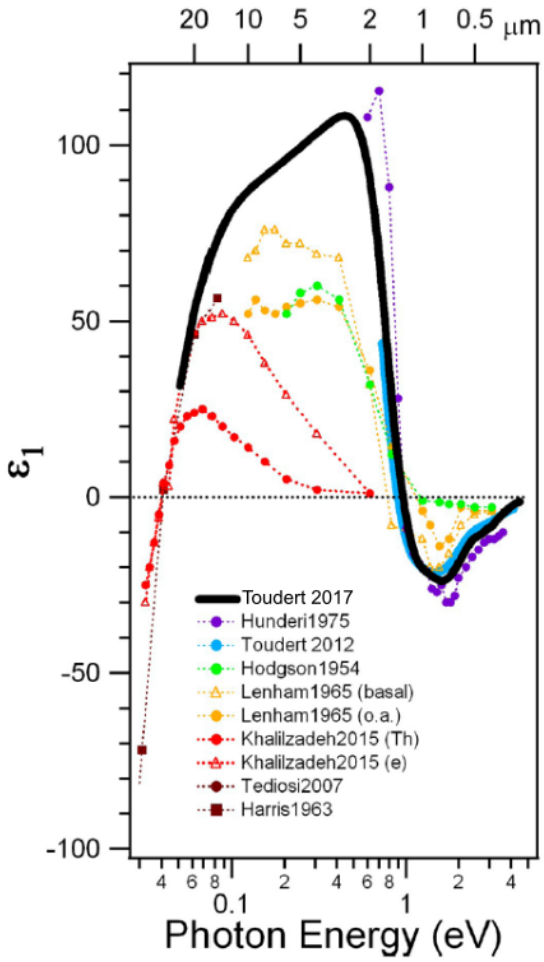

Figure 5. (colour) Ø. S. Handegård *et al.*

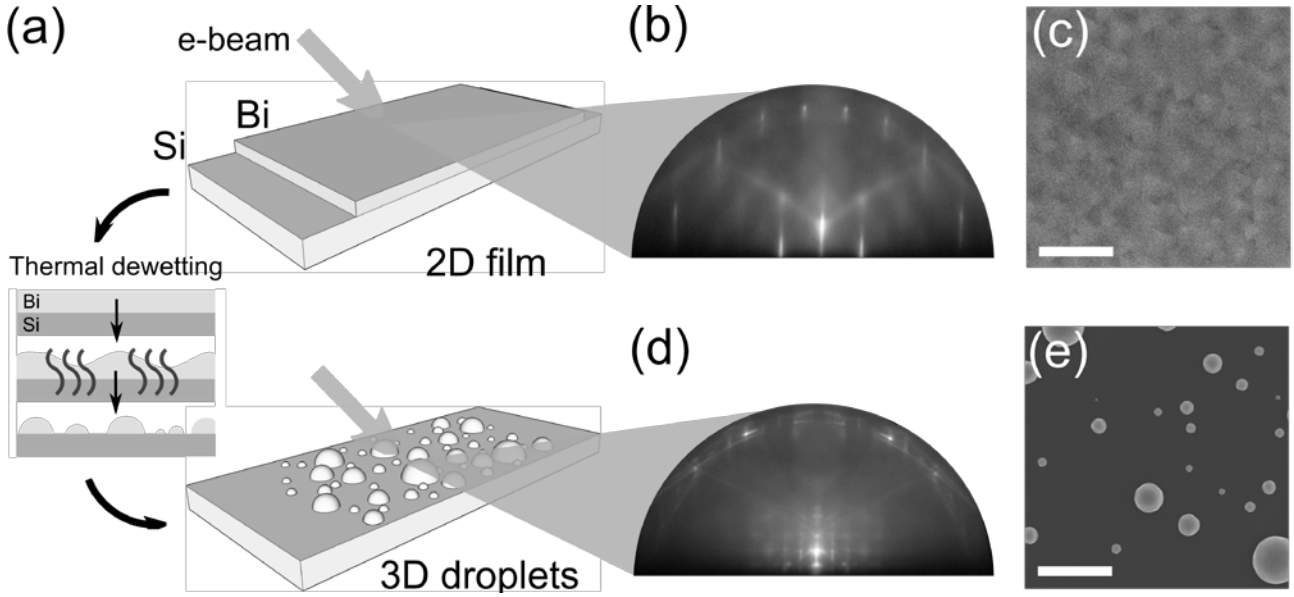

Figure 6. (greyscale) Ø. S. Handegård *et al.*

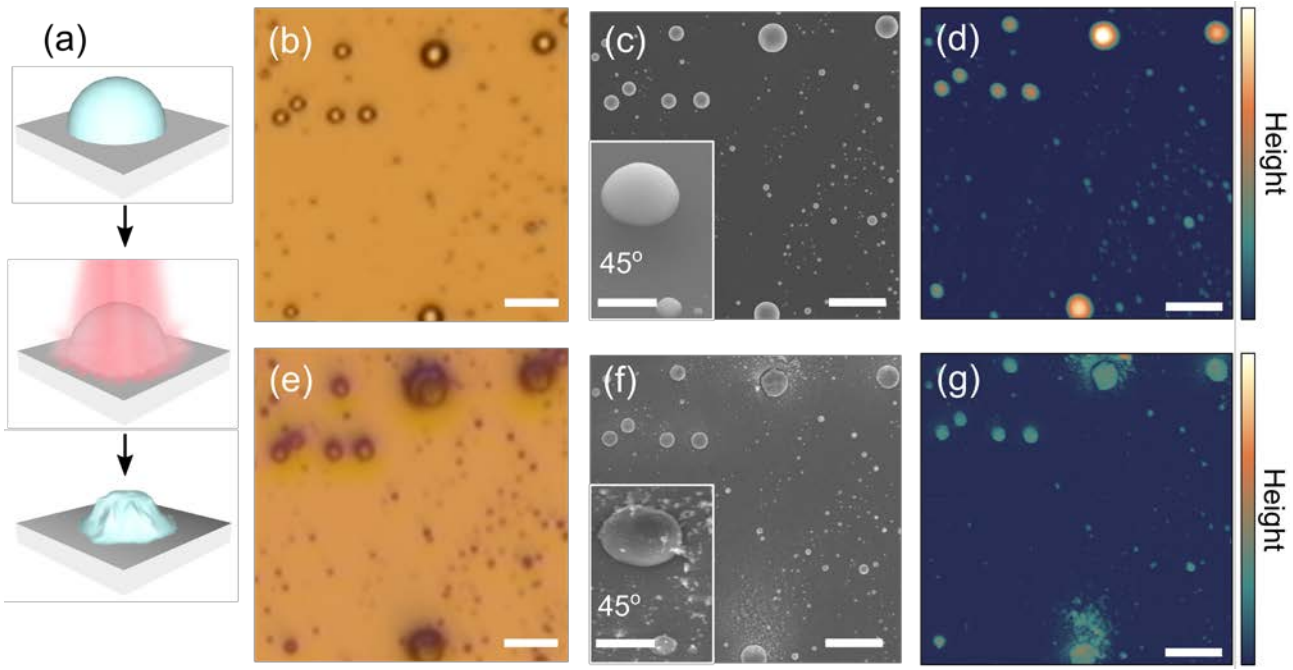

Figure. 7. (colour) Ø. S. Handegård *et al.*

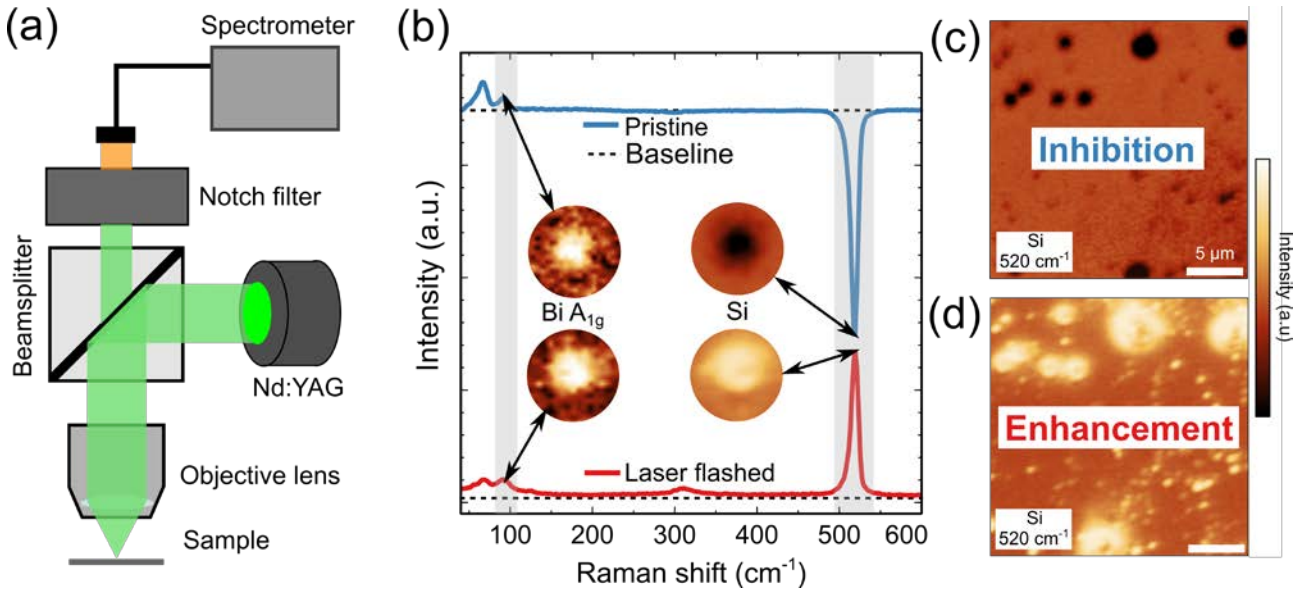

Figure 8. (colour) Ø. S. Handegård *et al.*

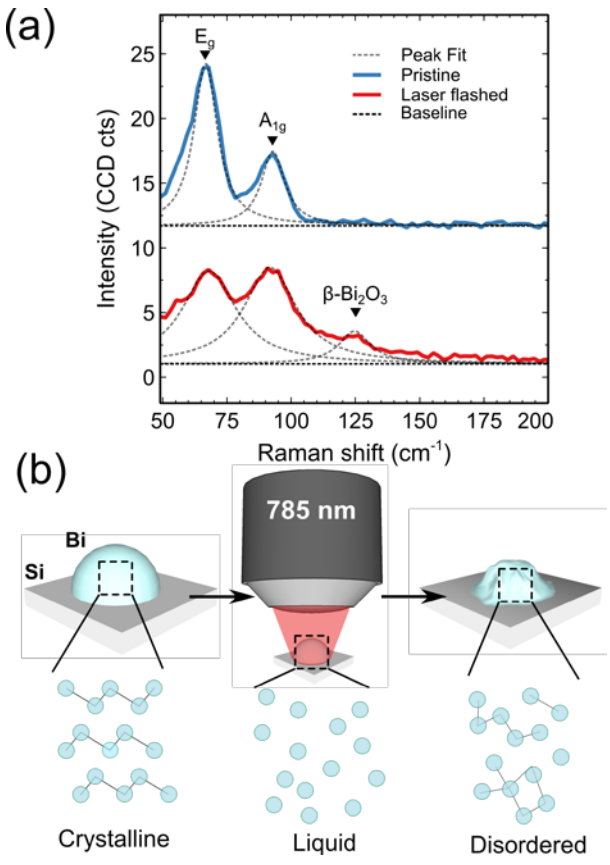

Figure 9. (colour) Ø. S. Handegård *et al.*

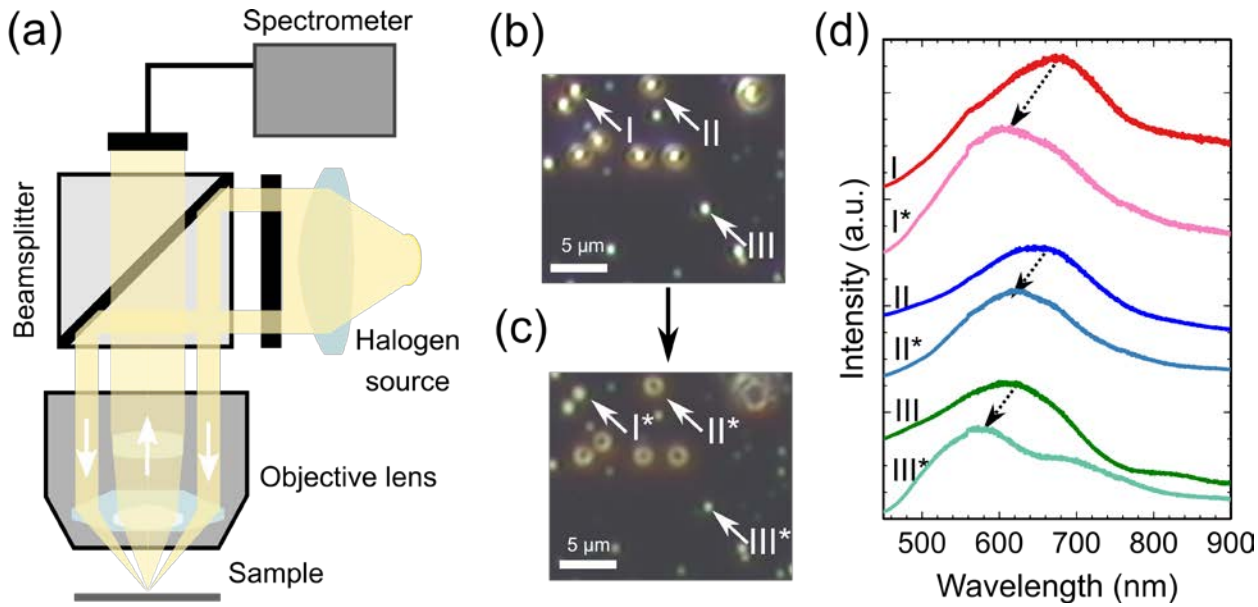

Figure 10. (colour) Ø. S. Handegård *et al.*